

Title no. 99-S56

Experimental Evaluation of Design Procedures for Shear Strength of Deep Reinforced Concrete Beams

by Gerardo Aguilar, Adolfo B. Matamoros, Gustavo J. Parra-Montesinos, Julio A. Ramírez, and James K. Wight

In this paper, results from the monotonic testing of four reinforced concrete deep beams are presented. The behavior of the deep beams is described in terms of cracking pattern, load-versus-deflection response, failure mode, and strains in steel reinforcement and concrete. Despite different failure modes, the failure loads and corresponding ultimate deflections were similar in all four specimens. Yielding of both longitudinal and transverse reinforcement occurred prior to failure. Based on the test results, the shear design procedures contained in the ACI 318-99 Code and Appendix A of the ACI 318-02 Code were evaluated. Both design procedures yielded conservative predictions of the shear strength of the single-span deep beams.

Keywords: beam; reinforced concrete; shear strength; strut; test.

INTRODUCTION

In this study, an evaluation was conducted of the behavior and strength of deep reinforced concrete beams based on results from the monotonic test of four beam specimens. The test specimens were designed with two different approaches, which consisted of: 1) the procedure described in Sections 10.7 and 11.8 of the ACI 318-99 Code (ACI Committee 318 1999); and 2) the Strut-and-Tie Method given in Appendix A of the ACI 318-02 Building Code (Cagley 2001), which is intended to replace the procedure given in Section 11.8 of the ACI 318-99 Code. The behavior of the deep beams is described in terms of cracking pattern, load-versus-deflection response, reinforcement and concrete strains, failure load, and failure mode. The experimental failure load of each specimen is compared with the load capacities calculated using the procedures given in the ACI 318-99 Code, and Appendix A of the ACI 318-02 Building Code.

RESEARCH SIGNIFICANCE

This paper presents experimental evidence that supports the use of the design procedures contained in Appendix A of the ACI 318-02 Code in reinforced concrete deep beams.

BACKGROUND

Over the past several decades, new approaches to the shear design of structural concrete have been implemented in codes of practice (Joint ACI-ASCE Committee 445 1998). One such procedure, the Strut-and-Tie Method (Schlaich, Schäfer, and Jennewein 1987), has already been incorporated into the AASHTO-LRFD Bridge Specifications and several international model codes (Joint ACI-ASCE Committee 445 1998). The strut-and-tie model (STM) procedure is widely used in the design of concrete regions where the distribution of longitudinal strains is significantly nonlinear, such as deep beams, beams with large openings, corbels, and dapped-end beams. Furthermore, the STM approach provides a unified framework for the extension of the ACI Code provisions to members and regions of members

not adequately covered by the existing code requirements, such as beams with large openings and beams loaded in the tension flange, amongst others.

SCOPE

The Reinforced Concrete Research Council (RCRC) supported this research to investigate and compare the behavior and strength of deep flexural members designed using Appendix A of the ACI 318-02 Building Code to that of members designed with the ACI 318-99 procedure in Section 11.8.

In this paper, a summary of the experimental work conducted as part of this research project is presented. A complete set of the experimental data is available elsewhere (Aguilar et al. 2002).

ACI 318-99 DEEP BEAM DESIGN

According to Section 11.8 of the ACI 318-99 Code, the sectional shear strength for deep flexural members is calculated by adding the contributions from the concrete and the distributed vertical and horizontal reinforcement. There are various expressions and limits for both the concrete and the steel contributions. The concrete contribution can be computed by using either Eq. (1) or Eq. (2)

$$V_c = \begin{cases} 2\sqrt{f'_c}b_wd \text{ (psi)} \\ \text{(Eq. (11-28), ACI 318-99 Code)} \\ \left(3.5 - 2.5\frac{M_u}{V_u d}\right)\left(1.9\sqrt{f'_c} + 2500\rho_w\frac{V_u d}{M_u}\right)b_wd \\ \text{less than } 6\sqrt{f'_c}b_wd \text{ (psi)} \\ \text{(Eq. (11-29), ACI 318-99 Code)} \end{cases} \quad (2)$$

where

$3.5 - 2.5(M_u)/(V_u d)$ is to be kept less than or equal to 2.5; and

f'_c = specified compressive strength of concrete, psi;

b_w = web width, in.;

d = effective depth (distance from extreme compression fiber to centroid of longitudinal tension reinforcement), in.;

V_u = factored shear force at the critical section, lb;

M_u = factored moment occurring simultaneously with V_u at the critical section, in.-lb. Critical section is located

ACI Structural Journal, V. 99, No. 4, July-August 2002.

MS No. 02-070 received September 25, 2001, and reviewed under Institute publication policies. Copyright © 2002, American Concrete Institute. All rights reserved, including the making of copies unless permission is obtained from the copyright proprietors. Pertinent discussion will be published in the May-June 2003 ACI Structural Journal if received by January 1, 2003.

Gerardo Aguilar is a PhD student in structural engineering at Purdue University, West Lafayette, Ind. His research interests include shear response and seismic behavior of reinforced concrete structures.

ACI member **Adolfo B. Matamoros** is an assistant professor of structures in the Department of Civil Engineering at the University of Kansas, Lawrence, Kans. He received his PhD from the University of Illinois at Urbana. He is Secretary of ACI Committee 408, Bond and Development of Reinforcement.

ACI member **Gustavo J. Parra-Montesinos** is an assistant professor at the University of Michigan, Ann Arbor, Mich., from which he received his PhD in 2000. He is a member of ACI Committee 335, Composite and Hybrid Structures. His research interests include the seismic behavior and rehabilitation of reinforced concrete and hybrid steel-concrete structures.

Julio A. Ramirez, FACI, is a professor and Assistant Head for Graduate Programs at the School of Civil Engineering, Purdue University. He is a member of ACI Committees 318, Structural Concrete Building Code; and 408, Bond and Development of Reinforcement; Joint ACI-ASCE Committees 423, Prestressed Concrete; and 445, Shear and Torsion; and the Technical Activities Committee. He received ACI's Delmar L. Bloem Award for Distinguished Service in 2000.

James K. Wight, FACI, is a professor of civil engineering at the University of Michigan. He is Chair of ACI Committee 318, Structural Concrete Building Code; and a member of Joint ACI-ASCE Committees 352, Joints and Connections in Monolithic Concrete Structures; and 445, Shear and Torsion. His research interests include earthquake-resistant design of reinforced concrete structures.

with respect to the face of support, at a distance $0.15l_n$ for uniformly loaded beams and at a distance $0.50a$ for beams with concentrated loads, but not to exceed d (Section 11.8.5, ACI 318-99 Code);

- $\rho_w = A_s/b_w d$ = ratio of web reinforcement;
 A_s = area of nonprestressed tension reinforcement, in.²;
 l_n = clear span measured face-to-face of supports, in.; and
 a = shear span (distance between concentrated load and face of support), in.

The use of shear reinforcement is required whenever the factored shear force at the critical section exceeds the shear strength $\phi V_c/2$ (Section 11.5.5.1, ACI 318-99 Code). The contribution from the shear reinforcement is computed with

$$V_s = \left[\frac{A_v}{s} \left(\frac{1 + l_n/d}{12} \right) + \frac{A_{vh}}{s_2} \left(\frac{11 - l_n/d}{12} \right) \right] f_y d \quad (\text{lb}) \quad (3)$$

(Eq. (11-30), ACI 318-99 Code)

where

- A_v = area of shear reinforcement perpendicular to flexural tension reinforcement within a distance s , in.²; and
 A_{vh} = area of shear reinforcement parallel to flexural tension reinforcement within a distance s_2 , in.²

It must be noted that, in the range of l_n/d values between 0 and 5, Eq. (3) apportions the contributions from the vertical and the horizontal reinforcement as a function of the geometry of the member. For the vertical reinforcement, the efficiency ranges between a theoretical minimum of 1/12 for $l_n/d = 0$ to a maximum of 1/2 for $l_n/d = 5$. On the other hand, the effectiveness of the horizontal reinforcement ranges from a maximum value of 11/12 for $l_n/d = 0$ to a minimum of 1/2 for $l_n/d = 5$. This clearly assumes a superior effectiveness of the distributed horizontal reinforcement in deep flexural members.

The ACI 318-99 Code defines an upper limit for the shear strength of deep flexural members

$$V_n \leq \begin{cases} 8\sqrt{f'_c} b_w d \text{ (psi)} & \text{for } \frac{l_n}{d} < 2 \\ \frac{2}{3} \left(10 + \frac{l_n}{d} \right) \sqrt{f'_c} b_w d \text{ (psi)} & \text{for } 2 \leq \frac{l_n}{d} \leq 5 \end{cases} \quad (4)$$

(Section 11.8.4, Eq. (11-27), ACI 318-99 Code)

The ACI 318-99 Code sets minimum amounts for both vertical and horizontal distributed reinforcement. Sections 11.8.9 and 11.8.10 of the ACI 318-99 Code state the following limits, respectively

$$A_v \geq 0.0015 b_w s; \quad s \leq \begin{cases} \frac{d}{5} \\ 18 \text{ in.} \end{cases} \quad (5)$$

$$A_{vh} \geq 0.0025 b_w s_2; \quad s_2 \leq \begin{cases} \frac{d}{3} \\ 18 \text{ in.} \end{cases} \quad (6)$$

The ACI 318-99 Code requires that the amount of shear reinforcement determined for the critical section be used throughout the span. Finally, regarding the anchorage of main longitudinal tension reinforcement into the supports, Sections 12.10.6 and 12.11.4 of the ACI 318-99 Code indicate that, at simple supports of deep flexural members, positive moment-tension reinforcement must be anchored to develop the specified yield strength f_y in tension at the face of the support.

APPENDIX A OF ACI 318-02 BUILDING CODE

Appendix A provides code language for the use of the STM in the design of structural concrete. In this study, STM, although applicable to various design situations, is used only for the design of deep flexural members. In the STM approach, the flow of forces or stresses within the member is represented by means of a truss system. Trusses consist of axially loaded elements in compression (struts) and tension (ties), and the intersections of the truss members are referred to as nodes. All struts, ties, and nodes have finite dimensions.

Appendix A includes a series of factors to be used as limiting values for the concrete stresses in struts β_s and nodes β_n . The limiting values are a function of the uniaxial concrete compressive strength and the strain conditions within the struts or at their ends. Values for β_s and β_n range from 0.6 to 1.0. Crack control, provided by the presence of a minimum amount of grid reinforcement in the struts, is taken into account by the β_s factor. For concrete compressive strengths not exceeding 6000 psi (41 MPa), a 25% increase (from 0.6 to 0.75) in the associated β_s factor is given for struts crossed by layers or grids of reinforcement parallel to the plane of the member that satisfies

$$\sum \frac{A_{si}}{b s_i} \sin \gamma_i \geq 0.003 \quad (7)$$

(Eq. (A-4), ACI 318-02 Code)

where
 A_{si} = area of surface reinforcement in the i -th layer crossing a strut, in.²;
 b = thickness of member, in.;
 s_i = spacing of reinforcement in the i -th layer adjacent to the surface of the member, in.; and
 γ_i = angle between the axis of a strut and the bars in the i -th layer of reinforcement crossing that strut.

A lower limit of 40 degrees for the angle γ_i is suggested when the reinforcement is provided in only one direction.

Specific requirements for the development of reinforcement are included in Appendix A. Development of hooks, headed reinforcing bars, mechanical anchorages, or straight bars should be provided at the nodes. The critical section for development is defined at the plane perpendicular to the tie where its centroid leaves the extended nodal zone.

EXPERIMENTAL PROGRAM

The experimental program was carried out at the Karl H. Kettelhut Structural Engineering Laboratory of the Purdue University School of Civil Engineering. It included the testing to failure of four full-scale deep reinforced concrete beams with different detailing schemes for the horizontal and vertical reinforcement. The design of the specimens and the actual testing was carried out jointly by researchers from Purdue University, the University of Michigan, and the University of Kansas. The details of the four beams tested in this study are described as follows.

TEST SPECIMENS

The four reinforced concrete beam specimens had an overall length of 176 in. (4470 mm), and were 36 in. (915 mm) deep and 12 in. (305 mm) wide. Figure 1 shows the general geometry and dimensions of the specimens. They were intended to represent deep members, for which it is plausible to envision a significant amount of the load carried directly from the load points to the supports by single compression struts. The specimens were designed as simply supported beams subjected to concentrated loads on the top face and supported on the

bottom face. Applied loads and support reactions were transmitted to the specimens by means of 12 x 12 x 2-in. (305 x 305 x 50 mm) steel plates. The shear span to effective depth ratio (a/d) was approximately 1.0.

According to ACI 318-99, Section 10.7.1, a beam is considered a deep flexural member for flexural design when the clear span-to-overall depth ratio l_n/h is less than 5/4 for simple spans. On the other hand, Section 11.8.1 specifies that deep beam action must be considered for shear design when the clear span-to-effective depth ratio l_n/d is less than 5.0, and the member is loaded on one face and supported on the opposite face so that struts can form between the loads and the supports. The specimens tested as part of this research project met the definition of deep flexural members for shear design as per Section 11.8.1. However, they did not satisfy the definition of a deep flexural member given in Section 10.7.1.

The four test specimens were labeled as ACI-I, STM-I, STM-H, and STM-M. The first three letters stand for the design approach used: ACI 318-99 Code (ACI) and Appendix A of the ACI 318-02 Code based on the STM. The second set of letters identifies whether the specimen was part of the first design group (I) with mechanical anchorages at ends of positive longitudinal reinforcement; the second group used 90-degree hooks at the ends of the positive longitudinal reinforcement (H); or used 90-degree hooks and had a modification to the minimum transverse reinforcement provision given in Appendix A (M).

SPECIMEN DESIGN PARAMETERS

For design purposes, 4000 psi (28 MPa) concrete compressive strength and 60 ksi (410 MPa) reinforcing steel yield strength were used. General design considerations for the four specimens are presented in Table 1. Figure 2 shows the reinforcement detailing used in the four specimens. The preliminary design of Specimens ACI-I, STM-I, and STM-H was carried out using the same factored point load of 175 kips (780 kN) placed at the third points of the span. A very small amount of vertical reinforcement was used in Specimen STM-M in an attempt to induce a compression failure of the strut between the load point and the support (Fig. 3). Only two vertical stirrups were placed within the shear span, as shown in Fig. 2. Table 2 summarizes the reinforcement detailing for the four test specimens.

Table 1—Design considerations

Beam no.	Specimen	Features
1	ACI-I	ACI 318-99 Code
		Mechanical anchorage
2	STM-I	Appendix A of ACI 318-02
		Mechanical anchorage
3	STM-H	Appendix A of ACI 318-02
		90-degree hook anchorage
4	STM-M	Reduced shear reinforcement in shear span
		90-degree hook anchorage

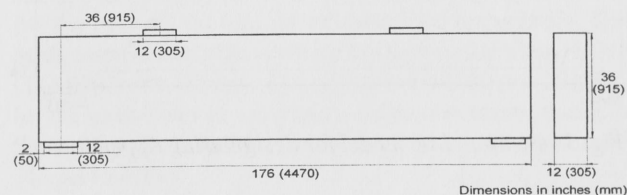


Fig. 1—Test specimen's elevation and cross section.

Table 2—Reinforcement of test specimens

Specimen	Vertical reinforcement		Horizontal reinforcement	Main tension longitudinal reinforcement	Main compression longitudinal reinforcement
	Shear span	Constant moment region			
ACI-I	No. 3 @ 6 in.	No. 3 @ 6 in.	No. 3 @ 4 in.	6 No. 8	2 No. 3
STM-I	No. 3 @ 6 in.	No. 3 @ 6 in.	No. 3 @ 12 in.	6 No. 8	2 No. 3
STM-H	No. 3 @ 6 in.	No. 3 @ 6 in.	2 No. 3	6 No. 8	2 No. 8
STM-M	2 No. 3	No. 3 @ 6 in.	None	6 No. 8	2 No. 8

Note: 1 in. = 25.4 mm

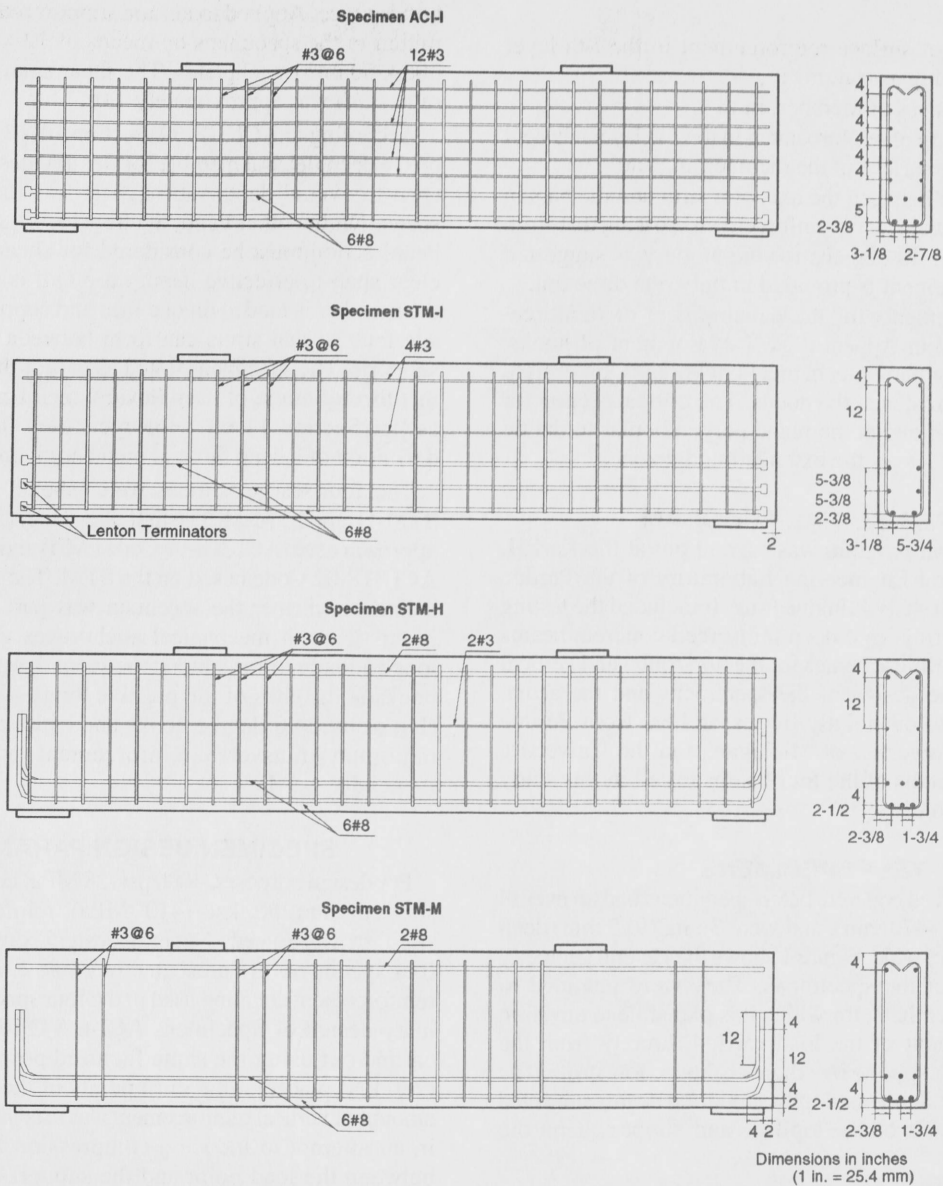


Fig. 2—Reinforcement detailing.

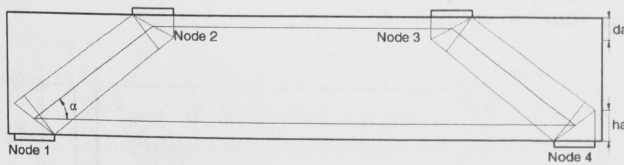


Fig. 3—Strut-and-tie model for design using Appendix A.

Main flexural steel

The main longitudinal tension reinforcement for the four specimens consisted of six No. 8, Grade 60 deformed bars. Two specimens, ACI-I and STM-I, had mechanical anchorages (terminators) at the ends of the positive moment longitudinal reinforcement. Figure 4 shows a view of such anchorage devices for both Specimen ACI-I and Specimen STM-I. The anchorage of the same reinforcement in the remaining two specimens was provided by standard 90-degree hooks. Specimen STM-H was built similarly to STM-I, except for a few modifications to the detailing scheme for the main longitudinal reinforcement (Fig. 2). Specimen STM-H

had two layers of main longitudinal tension reinforcement instead of the three layers used in STM-I. In STM-H, No. 8 deformed bars were used as compression reinforcement instead of the No. 3 bars used in Specimen STM-I. Specimen STM-M had the same longitudinal reinforcement as Specimen STM-H.

It is important to observe that the amount of main tension reinforcement in the ACI-I specimen was determined using standard flexural theory. For Specimen STM-I, the STM approach, using the truss model shown in Fig. 3, required the same longitudinal reinforcement.

Vertical and horizontal web reinforcement

The vertical reinforcement consisted of U-shaped, No. 3 deformed bars. The orientation of the open side of this reinforcement was alternated from top to bottom. The beam cross sections shown in all figures illustrate the case of the free ends of the stirrup being placed at the top of the reinforcement cage. The distributed horizontal steel also consisted of No. 3 bars.

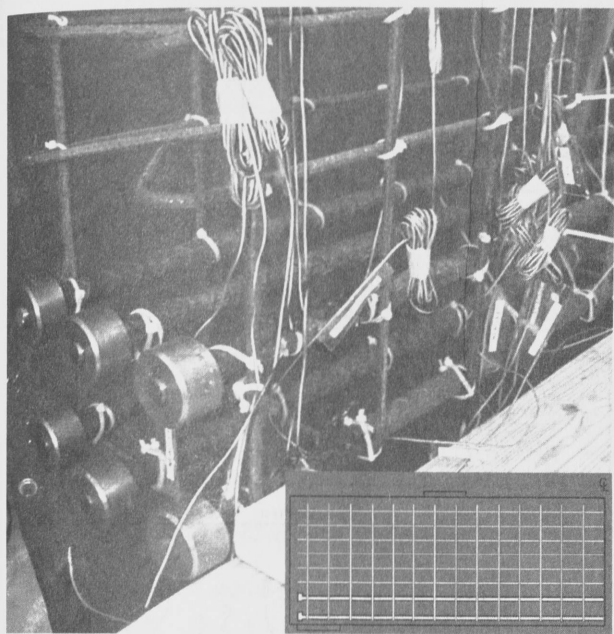


Fig. 4—Mechanical anchorage of longitudinal tension reinforcement.

The amount of distributed horizontal web reinforcement in Specimen ACI-I was significantly different from that used in the STM specimens, as shown in Table 2. The distributed reinforcement in the web for the ACI-I specimen was calculated on the basis of transverse shear requirements (Eq. (3)). The distributed, vertical, and horizontal web reinforcement of Specimens STM-I and STM-H was provided as per Eq. (7) to control crack growth along the main diagonal strut in the web of the member. In this study, the reinforcement specified by Eq. (7) was provided at a spacing not exceeding 12 in. or $0.5d$, measured perpendicular to the bars. The main load-carrying mechanism in the STM approach consisted of single diagonal struts between the loading and the support plates (Fig. 3). The limiting stress for the strut design was controlled by Section A.3.2 of Appendix A, which yielded a lower value than that of the effective compressive strength of the concrete in the nodal zone from Section A.5.2 at both ends of the struts. The differences between the two design approaches clearly supported the need for physical testing to evaluate the behavior and shear strength of these specimens.

A key issue studied in the experimental phase of this research was the adequacy of Eq. (3) for the determination of the required amount of vertical and distributed horizontal reinforcement. This equation indicates that the contribution of the vertical steel is to be significantly discounted in the low range of l_n/d values (10 to 30% effectiveness in the range l_n/d between 0.2 and 3.0). Conversely, it assigns a much higher effectiveness to the distributed horizontal reinforcement in the same range of l_n/d values (90 to 70%). All the specimens had an l_n/d ratio of 4.8, and Eq. (3) assigned a roughly equal effectiveness to both horizontal and vertical reinforcement.

In Specimen ACI-I, the vertical reinforcement was proportioned using the minimum amount permitted in Section 11.8.9, and the required additional strength was obtained by proportioning the distributed horizontal reinforcement using Eq. (3). This approach resulted in the detailing shown in Fig. 2.



Fig. 5—Cast and curing operations.

MATERIALS

All materials used in the construction of the specimens were sampled to determine their key mechanical properties. Concrete was obtained from a local ready-mix supplier. Volumetric proportioning and a 4-in. slump were used in the design of the 4000-psi (28 MPa) concrete mix. The first two specimens (ACI-I and STM-I) were cast from the same batch. A second batch, with a similar proportioning, was used in the last two specimens (STM-H and STM-M). For each batch, 6 in.-diameter cylinders and 6 x 6 in. beams were taken for later evaluation of properties.

The mechanical properties of the concrete were evaluated through standard tests. Three cylinders were tested 7 days after casting, four at 14 days, and four at 21 days. Six cylinders were tested 28 days after casting, and six more were tested the day of the deep beam test. The mean concrete compressive strength at 28 days was 4570 and 4100 psi (32 and 28 MPa) for the first and second pair of specimens, respectively. The mean concrete compressive strength at the test date was 4750 psi (33 MPa) for the first pair of specimens and 4130 psi (28 MPa) for the second pair of specimens. Beam specimens, tested in flexure, from both batches gave a mean modulus of rupture of 715 psi (5 MPa).

All reinforcement of a given size was obtained from the same heat. The reinforcing steel was randomly sampled. Three coupons for each bar diameter were extracted and tested monotonically to failure. Tensile tests showed that the mean yield stress was 65 ksi (450 MPa) for the No. 3 bars, and 61 ksi (420 MPa) for the No. 8 bars. The ultimate strengths for the No. 3 and No. 8 bars were 104 and 101 ksi (720 and 700 MPa), respectively.

The specimens were cast following common procedures, wet-cured for seven days, and then removed from their wood formwork. Figure 5 shows some aspects of the casting and curing operations.

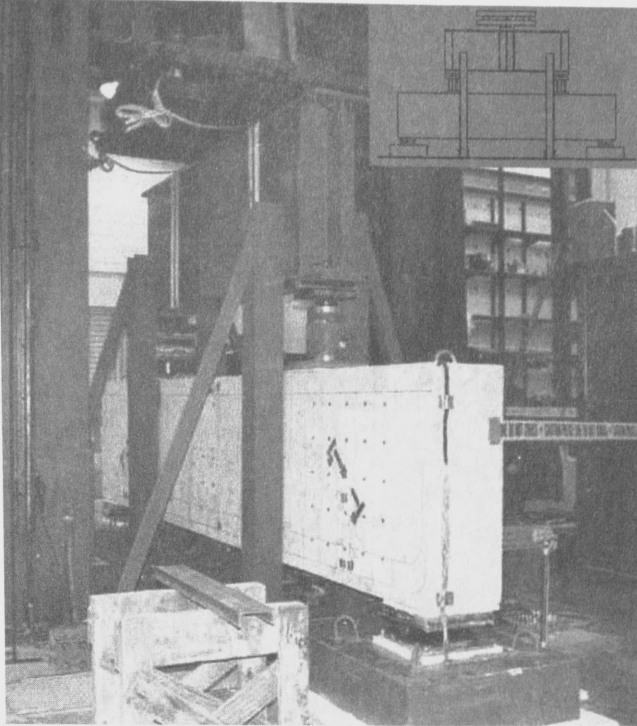
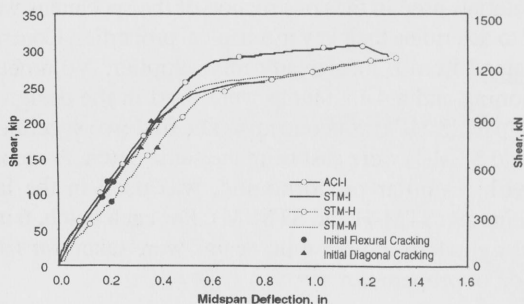


Fig. 6—Setup in loading frame.



Specimen	Initial Flexural Cracking		Initial Diagonal Cracking		Failure		Mode of Failure
	V, kip	Δ , in.	V, kip	Δ , in.	V, kip	Δ , in.	
ACI-I	120	0.22	200	0.39	305	1.24	Flexure
STM-I	120	0.23	200	0.38	255	0.80 ¹	Flexure
STM-H	85	0.20	160	0.38	289	1.32	Shear
STM-M	95	0.17	160	0.32	287	1.27	Shear

¹ Measurements stopped before failure

1 kip = 4.448 kN
1 in = 25.4 mm

Fig. 7—Comparison of shear force-deflection curves for test specimens.

TEST SETUP AND INSTRUMENTATION

The test setup is shown in Fig. 6. Symmetric point loads were applied using a 600 kip (2670 kN) universal testing machine and a spreader beam. Pin-and-roller supports were approximated with 2 in.-diameter (50 mm) steel rods between two 2 in.-thick (50 mm), 12 in.-square (305 mm) steel plates. The rods and steel plates permitted the placement of concentrated loads at the desired locations. The load was monitored by placing two load cells on the top faces of the specimens. Nine displacement transducers were mounted at the support locations and throughout the span to monitor deflections. The load was applied monotonically up to failure, pausing at key behavior points to mark cracks, collect data from various instrumentation devices, and take photographs.

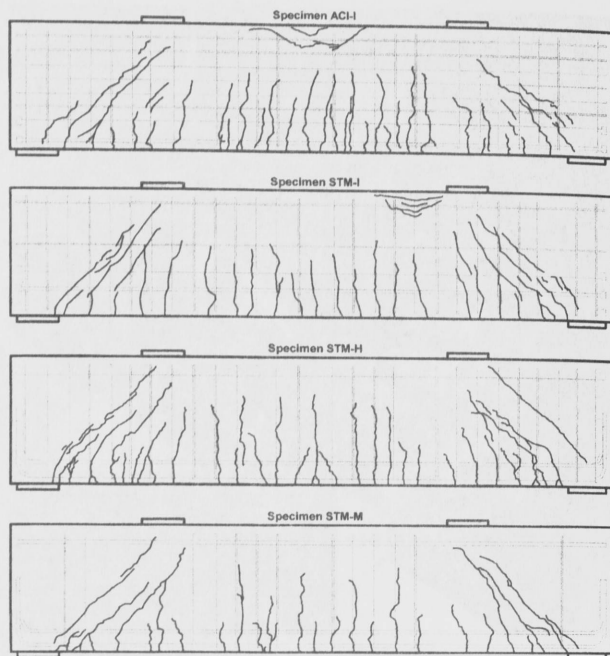


Fig. 8—Final crack patterns.

To monitor the behavior of the test specimens, approximately 40 electric strain gages were attached to the longitudinal and transverse reinforcement at key locations for each specimen. In addition, concrete surface-strain gages were placed in the shear spans and between load points. Whittemore points were glued to one of the lateral faces of the beams within the shear span, as well as between point loads. A PC-based data acquisition system was used to monitor and record data during the tests.

BEHAVIOR OF TEST BEAMS

Load-deflection relationships

The load-deflection behavior of each specimen is shown in Fig. 7. All four specimens exhibited similar overall behavior, which was characterized by a nearly bilinear response. Companion specimens ACI-I and STM-I had similar diagonal tension-cracking strength. This was also true for companion specimens STM-H and STM-M. After flexural cracking, a second, softer linear region was observed in all of the specimens up to the first yielding of the main longitudinal reinforcement. This was followed by a plateau extending to failure.

Failure modes

The critical shear crack, later becoming the failure crack, formed at approximately the same load for all specimens (approximately 240 kips [1070 kN]). The orientation of these cracks was somehow controlled by the geometry of the shear span and the dimensions of the support and loading areas. Failure of the specimens took place only after the primary diagonal crack developed fully between the load and support regions, and after yielding of main tension reinforcement. Significant splitting within the shear span, noted as cracks parallel to the axis of the main struts, was observed for all specimens. At failure, some crushing of the compression zone at midspan was observed. In Specimens ACI-I and STM-I, which failed in flexure, the crushing covered a relatively large region between point loads. Specimens STM-H and STM-M failed in shear compression. Figure 8 shows the sketches

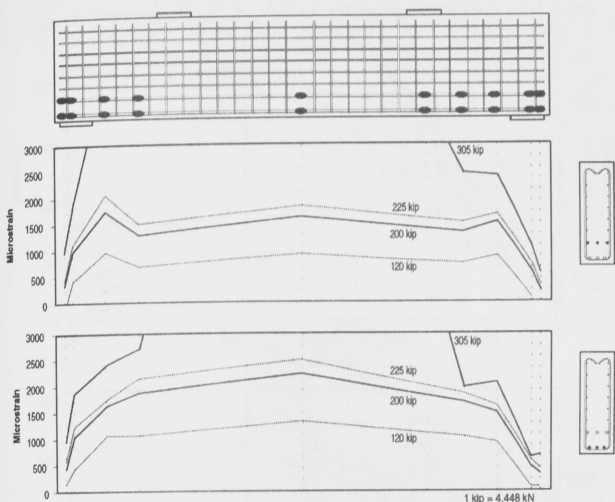


Fig. 9—Longitudinal reinforcement strains (Specimen ACI-I).

corresponding to the crack patterns just before failure for all four specimens.

Longitudinal reinforcement strains

The distribution of strains along the main longitudinal reinforcement, determined from electric strain gages, was recorded during the tests. Strain distributions at various stages of loading are presented in Fig. 9 through 11. The strain distributions corresponding to Specimen STM-I, which are not presented, were very similar to those of Specimen ACI-I. The strain distributions for each plot correspond to shear force at initial flexural cracking, first diagonal cracking, first yield of longitudinal reinforcement, and failure. To facilitate comparison, the plotted values of strain were limited to a maximum of 3000 microstrain, although higher strains were recorded at some locations.

As can be seen in Fig. 9 through 11, the strain distributions for all specimens were similar. They are roughly symmetric, with increasing strains towards midspan. For all four specimens, regardless of the type of anchorage, a rapid reduction in reinforcement strain was observed between the inner edge of the support plate (towards the shear span) and the back side of the plate (towards the end of the beam). Near the end of the test, strains in excess of yield were recorded at the face of the support-bearing plate. Throughout the loading operation of all specimens, a roughly constant distribution of strains was recorded from face to face of the support-bearing plates, a result that is consistent with the STM design approach.

The strain measurements highlight the inconsistency resulting from two different definitions for deep flexural members in the ACI 318-99 Code. The tested members exhibited deep beam action characterized by high strains, and hence, high stresses, in the main flexural-tension reinforcement almost all the way into the support. On the other hand, the significant drop in strain through the bearing area indicates a beneficial condition for anchorage of this reinforcement. This is not currently reflected in the anchorage requirements given in the ACI 318-99 Code.

Vertical reinforcement strains

Vertical reinforcement strains at two different points on a stirrup leg were recorded during the tests. Figure 12 shows the average strain at each instrumented stirrup. The readings are shown for four shear-force stages corresponding to initial flexural cracking, first diagonal cracking, first yield of

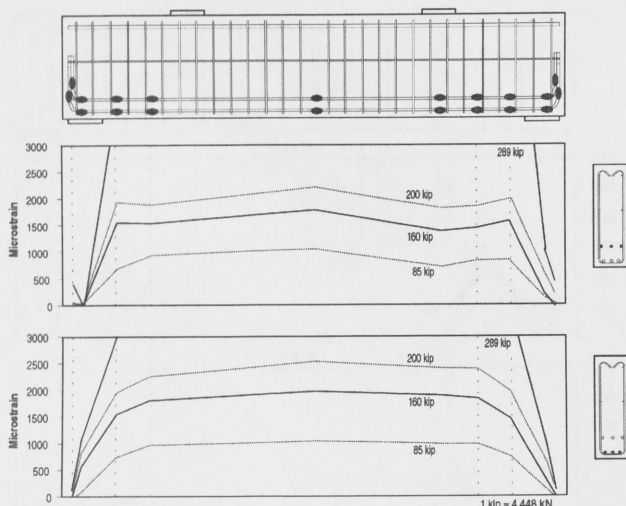


Fig. 10—Longitudinal reinforcement strains (Specimen STM-H).

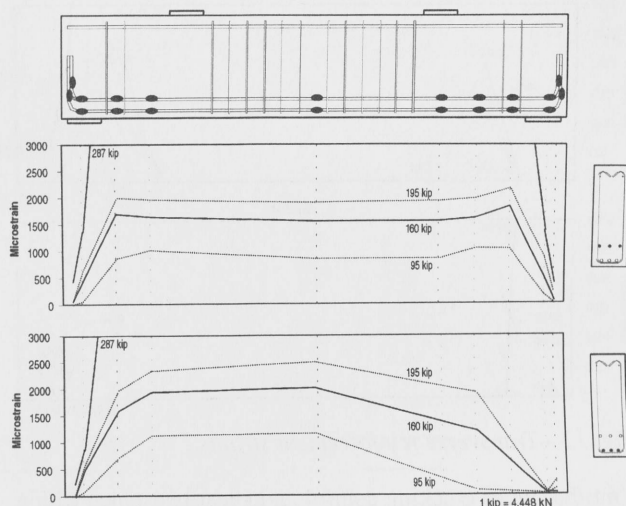


Fig. 11—Longitudinal reinforcement strains (Specimen STM-M).

longitudinal reinforcement, and failure. Again, plots are limited to 3000 microstrain for purposes of clarity.

The plots for Specimens ACI-I, STM-I, and STM-H were relatively similar. The strain readings in the stirrup legs were sensitive to the relative location of the strain gages with respect to the diagonal cracks. As shown in Fig. 12, large strain readings concentrated primarily in one or two stirrups, for which the gage location was either crossed by or near a diagonal crack within the shear span. This is in agreement with the findings of previous researchers (Anderson and Ramirez 1989), indicating that the efficiency of the transverse reinforcement is highly dependent on its relative location with respect to the crack pattern (Fig. 8). This observation supports the detailing practice of distributing the vertical reinforcement uniformly, given the uncertainty associated with the location and geometry of diagonal shear cracking. This uncertainty decreases, however, for deep beams loaded with a concentrated load on one face and supported on the opposite face.

At load levels close to failure, tensile strains of 0.0015 or higher were monitored in selected stirrups of all four specimens, indicating that vertical transverse reinforcement was actively

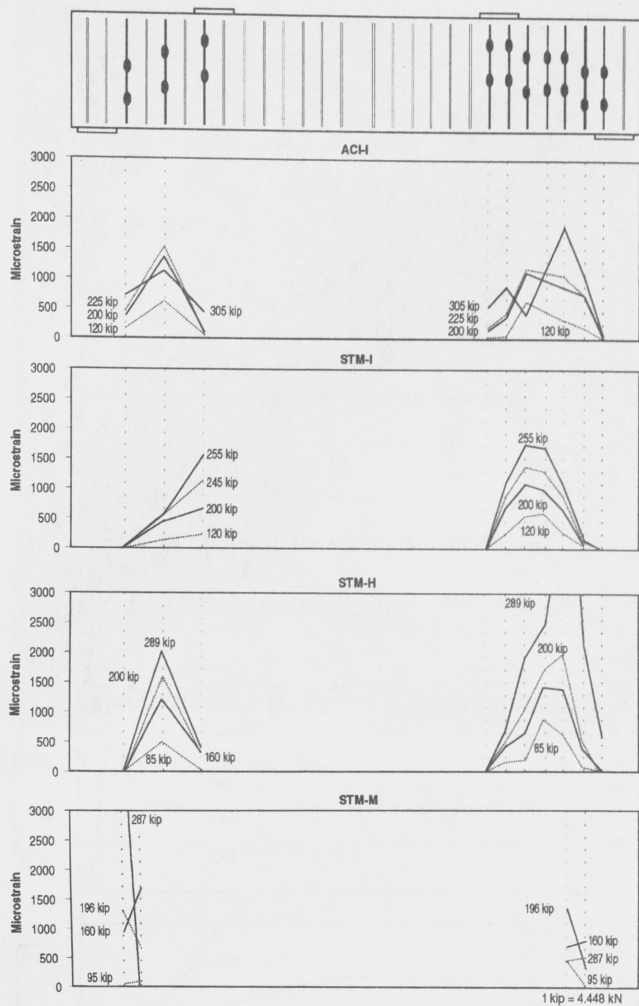


Fig. 12—Transverse reinforcement strains.

contributing to cracking control and shear resistance within the shear span.

Measured concrete strains

Concrete is not an ideal material for the application of electrical strain gages, and the accuracy of local measurement with these gages is limited. Surface gages 2 in. (50 mm) and larger, however, have been used with some degree of success at the Kettlehut Laboratory. In this study, 2 in. (50 mm) electrical strain gages were used to determine concrete strains in the constant moment region and in the shear span. Figure 13 illustrates the progression of surface concrete strains with increasing shear force for two locations at midspan in Specimens STM-I, STM-H, and STM-M.

The measured values of concrete strain at failure in the flexural compression zone ranged between 0.001 and 0.003. No relationship could be established between the mode of failure and the maximum surface strains recorded at midspan. Various investigations have assigned values ranging from 0.003 to 0.004 to the concrete strain associated with first crushing in flexure, depending on the instrumentation and type of loading used in the tests. Under different conditions of stressing, such as near heavily loaded bearing zones where failures initiated in these specimens, the magnitude of strain associated with concrete crushing may be quite different.

In all four specimens, large inelastic deformations were recorded at midspan prior to failure, particularly in

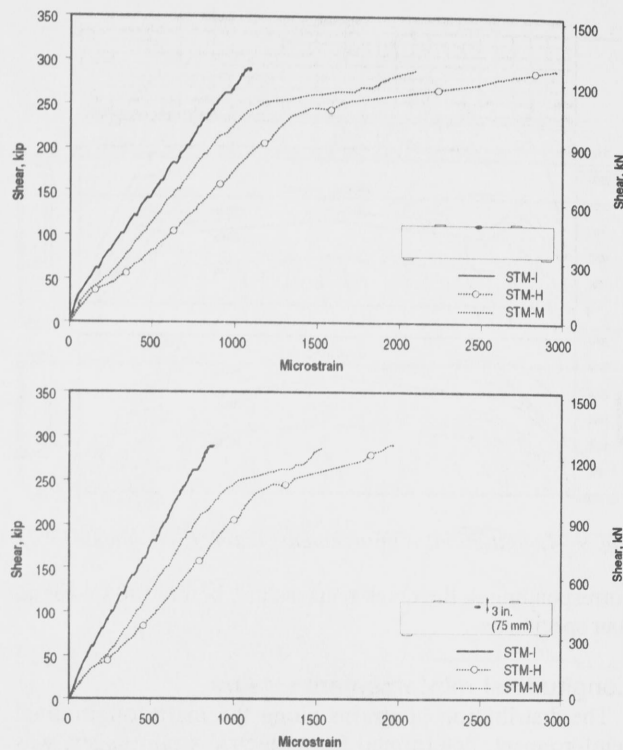


Fig. 13—Strains at midspan (surface electric strain gages).

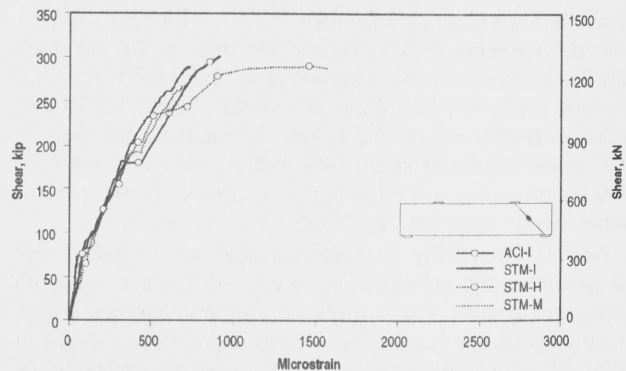


Fig. 14—Strains along struts (surface electric strain gages).

Specimen STM-I, which exhibited some rigid-body rotation about one of its supports. Concrete strains at 3 in. (75 mm) from the top surface of the beams were observed to be approximately 70% of those at the top face (Fig. 13). This proportion was approximately constant for all specimens throughout the tests.

Figure 14 shows the relationship between shear force and concrete surface strain on a diagonal line between the center of the loading point and the center of the support plates for the four specimens. This diagonal line simulates the main load-carrying strut assumed in the STM design (Fig. 3). The four graphs follow a similar trend, except for a sudden increase in strain at failure for Specimen STM-H.

For safety reasons, concrete strain measurements by means of a 6-in. (150 mm) gage length LVDT were not carried out to failure. Figure 15 shows the relationship between shear force and surface strain at midspan. The strain distributions over the depth at midspan indicate an approximately linear trend for all four measurements recorded prior to yielding of the main longitudinal reinforcement.

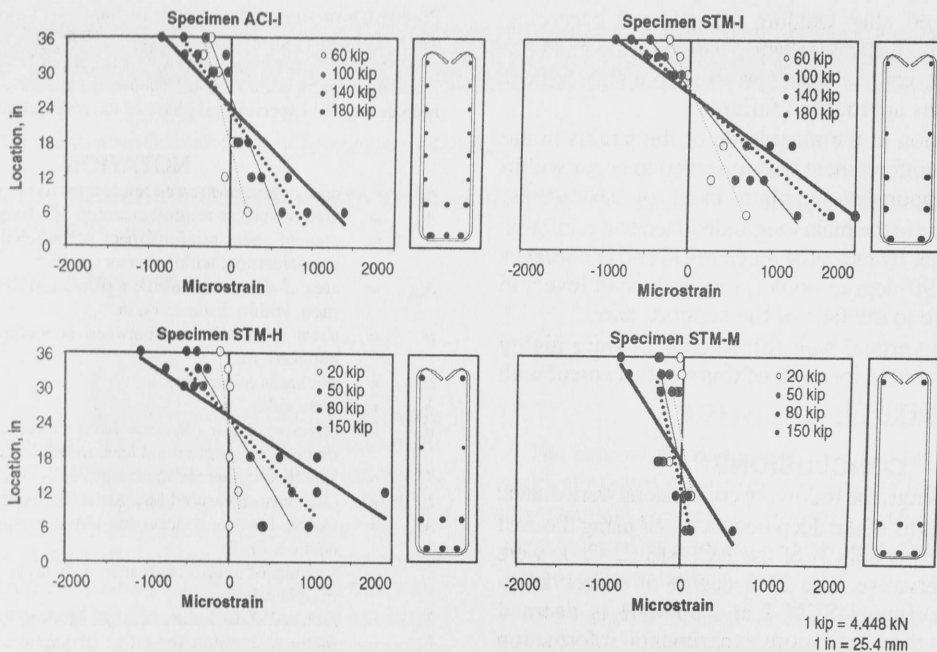


Fig. 15—Strains at midspan (6-in. [150 m] LVDT gage).

Table 3—Measured and calculated capacities

Specimen	Measured shear capacity V_M , kips	Calculated capacities, kips							
		Nominal properties				Measured properties			
		ACI, V_{ACI}	STM, V_{STM}	$\frac{V_{ACI}}{V_M}$	$\frac{V_{STM}}{V_M}$	ACI, V_{ACI}	STM, V_{STM}	$\frac{V_{ACI}}{V_M}$	$\frac{V_{STM}}{V_M}$
ACI-I	305	169	186	0.55	0.61	214	226	0.70	0.74
STM-I	255	106	166	0.42	0.65	133	203	0.52	0.80
STM-H	289	126	188	0.44	0.65	152	225	0.53	0.78
STM-M	287	98	153	0.34	0.53	117	186	0.41	0.65
Average	—	—	—	0.44	0.61	—	—	0.54	0.74

Note: 1 kip = 4.448 kN

COMPARISON OF MEASURED AND DESIGN CAPACITIES

A comparison between the measured and calculated shear capacities of the specimens was carried out. The shear capacity for all specimens was calculated using both nominal and measured material properties. No strength-reduction factor was used when calculating specimen capacities. Two approaches were used: 1) the ACI 318-99 Code; and 2) Appendix A of the ACI 318-02 Code using a four-node statically determined truss model (Fig. 3). Table 3 summarizes the results of this comparison.

It is evident that the shear capacities calculated by both the ACI 318-99 Code and Appendix A are very conservative. The ACI 318-99 Code, which is based on empirical equations, is more conservative than the STM approach, which considers a more realistic representation of the load-carrying mechanism in deep flexural members. This assertion is further supported by the measured capacity of Specimen STM-M. The detailing of this specimen, although not recommended for practice, clearly demonstrates the fallacy of assigning effectiveness to the distributed vertical and horizontal reinforcements on the basis of Eq. (3). This specimen, without distributed horizontal reinforcement throughout the web, and with concentrated vertical reinforcement in the form of two stirrups, showed the ability of the deep beam to carry load primarily

by a single strut mechanism between the load and support points. It must be pointed out that the load-carrying mechanism of Specimen STM-M probably included both the participation of the transverse reinforcement and the dowel action of the main longitudinal reinforcement.

SUMMARY OF FINDINGS AND CONCLUSIONS

Four deep beams were monotonically tested to failure to evaluate the adequacy of Appendix A of the 2002 edition of the ACI 318 Code for the design of deep flexural members. The test specimens were subjected to third-point loads in addition to their self-weight. At failure, all specimens exhibited a primary diagonal crack running from the support region to the point load. Some crushing of the concrete in the flexural compression zone near the loading plate was observed in all specimens. Specimens ACI-I and STM-I failed in flexure. Specimens STM-H and STM-M failed in shear compression. Based on the analysis of the test results, the following observations were made:

1. Despite the different modes of failure, failure loads, and corresponding ultimate deflections for Specimens ACI-I, STM-H, and STM-M, they were within 6% of each other. Specimen STM-I recorded the smallest load and deflection at failure;

2. Failure occurred after yielding (strain level exceeding 0.0021) of both longitudinal and transverse reinforcement. Large strains were locally recorded in the vertical web reinforcement as all four specimens approached failure;

3. A large reduction in the magnitude of the strains in the main longitudinal reinforcement was observed to occur within the length of the support-bearing plates in all four specimens;

4. Recorded strains in the main longitudinal tension reinforcement, anchored either by means of mechanical end anchorages or using standard 90-degree hooks, reached yield levels in the shear span close to the face of the support; and

5. Strains in the vertical web reinforcement were highly dependent on the relative location of this reinforcement with respect to the crack pattern.

CONCLUSIONS

Based on the findings, the following conclusions were drawn:

1. The shear designs of the deep beams tested using the ACI 318-99 Code and Appendix A of the ACI 318-02 Code were shown to be conservative. The 25% degree of conservatism observed for Specimens STM-I and STM-H is deemed appropriate at this time until more experimental information is available. This represents a significant improvement over the current ACI method that resulted in a test load of almost two times the calculated value;

2. Provisions for proportioning the vertical and distributed horizontal reinforcement in the web according to Section 11.8.8 of the ACI 318-99 Code did not properly reflect the overall behavior of the test specimens. The STM gives a better representation of the load-carrying mechanism at failure in deep flexural members, and leads to reductions in the amount of distributed vertical and horizontal reinforcement; and

3. The significant reduction in the magnitude of strains measured in the main longitudinal tension reinforcement over the length of the support-bearing plate indicates a favorable anchorage condition in these highly compressed regions of a deep flexural member. This condition is not presently acknowledged in the ACI 318-99 Code.

ACKNOWLEDGMENTS

This study was conducted in the Karl H. Kettlehut Structural Engineering Laboratory at Purdue University under the sponsorship of the Reinforced Concrete Research Council. The support of the Erico Corporation, through the donation of the longitudinal reinforcement and the Lenton terminators for Specimens ACI-I and STM-I is also recognized. Thanks are extended to

Purdue University graduate students Santiago Pujol and Koray Tureyen; undergraduate students James Reisert, Dave Blackman, and Kyle Fisher; postdoctoral research assistant Lisa Samples; and to University of Michigan graduate students Burcu Burak, Xuemei Liang, and Afsin Canbolat for their help during the experimental phase of the research project.

NOTATION

A_s	=	area of nonprestressed tension reinforcement, in. ²
A_{si}	=	area of surface reinforcement in i -th layer crossing strut, in. ²
A_v	=	area of shear reinforcement perpendicular to flexural tension reinforcement within distance s , in. ²
A_{vh}	=	area of shear reinforcement parallel to flexural tension reinforcement within distance s_2 , in. ²
a	=	shear span (distance between concentrated load and face of support), in.
b	=	thickness of member, in.
b_w	=	web width, in.
d	=	effective depth (distance from extreme compression fiber to centroid of longitudinal tension reinforcement), in.
f'_c	=	specified compressive strength of concrete, psi
l_n	=	clear span measured face-to-face of supports, in.
M_u	=	factored moment occurring simultaneously with V_u at critical section, in.-lb
s_i	=	spacing of reinforcement in i -th layer adjacent to surface of member, in.
V_u	=	factored shear force at critical section, lb
β_n	=	factor to account for effect of anchorage of ties on effective compressive strength of nodal zone
β_s	=	factor to account for effect of cracking and confining reinforcement on effective compressive strength of concrete in strut
γ_i	=	angle between axis of strut and bars in i -th layer of reinforcement crossing that strut
ρ_w	=	ratio of web reinforcement

REFERENCES

- ACI Committee 318, 1999, "Building Code Requirements for Structural Concrete (ACI 318-99) and Commentary (318R-99)," American Concrete Institute, Farmington Hills, Mich., 391 pp.
- Aguilar, G.; Matamoros, A.; Parra-Montesinos, G.; Ramirez, J. A.; and Wight, J. K., 2002, "Experimental and Analytical Evaluation of Design Procedures for Shear Strength of Deep Reinforced Concrete Beams," *Civil Engineering Report*, Purdue University, West Lafayette, Ind.
- American Association of State Highway and Transportation Officials, 1994, *Standard Specifications for Highway Bridges*, 16th Edition.
- Anderson, N. S., and Ramirez, J. A., 1989, "Detailing of Stirrup Reinforcement," *ACI Structural Journal*, V. 86, No. 5, Sept.-Oct., pp. 507-515. (also errata, V. 86, No. 6, Nov.-Dec., p. 767).
- Cagley, J. R., 2001, "Changing from ACI 318-99 to ACI 318-02—What's New?," *Concrete International*, V. 23, No. 6, June, pp. 69-184.
- Joint ACI-ASCE Committee 445, 1998, "Recent Approaches to Shear Design of Structural Concrete," *Journal of Structural Engineering*, ASCE, V. 124, No. 12, Dec., pp. 1375-1417.
- Schlaich, J.; Schäfer, K.; and Jennewein, M., 1987, "Toward a Consistent Design of Structural Concrete," *PCI Journal*, V. 23, No. 3, May-June, pp. 74-150.